

DTIC FILE COPY

4

GL-TR-89-0318

DETERMINATION OF THE GRAVITY DISTURBANCE BY PROCESSING THE GRAVITY GRADIOMETER SURVEYING SYSTEM - PROCESSING PROCEDURE AND RESULTS

Yan Ming Wang

DEPARTMENT OF GEODETIC SCIENCE AND SURVEYING
THE OHIO STATE UNIVERSITY
COLUMBUS, OHIO 43210

AD-A219 992

August 1989

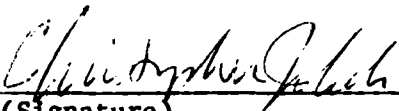
SCIENTIFIC REPORT NO. 8


APPROVED FOR PUBLIC RELEASE; DISTRIBUTION UNLIMITED

DTIC
ELECTE
APR 02 1990
S E D
VO

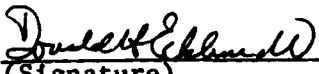
GEOPHYSICS LABORATORY
AIR FORCE SYSTEMS COMMAND
UNITED STATES AIR FORCE
HANSCOM AIR FORCE BASE, MASSACHUSETTS 01731-5000

"This technical report has been reviewed and is approved for publication"


(Signature)
CHRISTOPHER JEKELI
Contract Manager


(Signature)
THOMAS ROONEY
Branch Chief

FOR THE COMMANDER


(Signature)
DONALD H. ECKHARDT
Division Director

This report has been reviewed by the ESD Public Affairs Office (PA) and is releasable to the National Technical Information Service (NTIS).

Qualified requestors may obtain additional copies from the Defense Technical Information Center. All others should apply to the National Technical Information Service.

If your address has changed, or if you wish to be removed from the mailing list, or if the addressee is no longer employed by your organization, please notify GL/IMA, Hanscom AFB, MA 01731. This will assist us in maintaining a current mailing list.

Do not return copies of this report unless contractual obligations or notices on a specific document requires that it be returned.

REPORT DOCUMENTATION PAGE

1a. REPORT SECURITY CLASSIFICATION Unclassified		1b. RESTRICTIVE MARKINGS	
2a. SECURITY CLASSIFICATION AUTHORITY		3. DISTRIBUTION / AVAILABILITY OF REPORT Approved for public release; distribution unlimited	
2b. DECLASSIFICATION / DOWNGRADING SCHEDULE		4. PERFORMING ORGANIZATION REPORT NUMBER(S) RF Project 765306/718188	
4. PERFORMING ORGANIZATION REPORT NUMBER(S) RF Project 765306/718188		5. MONITORING ORGANIZATION REPORT NUMBER(S) GL-TR-89- 0318	
6a. NAME OF PERFORMING ORGANIZATION Department of Geodetic Science and Surveying	6b. OFFICE SYMBOL (if applicable) DGSS	7a. NAME OF MONITORING ORGANIZATION Geophysics Laboratory	
6c. ADDRESS (City, State, and ZIP Code) The Ohio State University Columbus, Ohio 43210		7b. ADDRESS (City, State, and ZIP Code) Hanscom AFB Massachusetts 01731-5000	
8a. NAME OF FUNDING / SPONSORING ORGANIZATION Air Force Geophysics Laboratory	8b. OFFICE SYMBOL (if applicable) AFGL	9. PROCUREMENT INSTRUMENT IDENTIFICATION NUMBER F-19628-86-K-0016	
8c. ADDRESS (City, State, and ZIP Code) Hanscom Air Force Base, Massachusetts 01731		10. SOURCE OF FUNDING NUMBERS	
		PROGRAM ELEMENT NO. 62101F	PROJECT NO. 7600
		TASK NO. 03	WORK UNIT ACCESSION NO. AQ
11. TITLE (Include Security Classification) Determination of the Gravity Disturbance by Processing the Gravity Gradiometer Surveying System - Processing Procedure and Results			
12. PERSONAL AUTHOR(S) Yan Ming Wang			
13a. TYPE OF REPORT Scientific No. 8	13b. TIME COVERED FROM _____ TO _____	14. DATE OF REPORT (Year, Month, Day) 1989, August	15. PAGE COUNT 30
16. SUPPLEMENTARY NOTATION			
17. COSATI CODES		18. SUBJECT TERMS (Continue on reverse if necessary and identify by block number)	
FIELD	GROUP	Gravity, Gradiometer, Gravity Gradiometer Surveying System	
19. ABSTRACT (Continue on reverse if necessary and identify by block number)			
<p>The gravity gradiometer surveying system (GGSS) took the first flight in the Texas/Oklahoma area and the data were released by Air Force Laboratory in April, 1989. The main problem of processing the GGSS gradient data is that there is bias in the data. If the tie point values of the gravity gradient are available, then the bias can be removed from the GGSS gradient data by using crossover discrepancy adjustment.</p> <p>Since there are no tie point values of the gravity gradient, the free-air gravity anomaly was used as the tie point values. Two components of the GGSS gradient data T_{xz} and T_{yz} were integrated linearly into the vertical derivatives of the disturbing potential T_z, the bias and tilt in the T_z for each track were removed by combining the tie point values of the free-air anomaly in the test area. Finally, the T_z was recovered on the ground by using the fast Fourier transformation and least squares collocation. The results were compared with the free-air anomalies in the test area. The</p>			
20. DISTRIBUTION / AVAILABILITY OF ABSTRACT <input checked="" type="checkbox"/> UNCLASSIFIED/UNLIMITED <input type="checkbox"/> SAME AS RPT <input type="checkbox"/> DTIC USERS		21. ABSTRACT SECURITY CLASSIFICATION Unclassified	
22a. NAME OF RESPONSIBLE INDIVIDUAL Christopher Jekeli		22b. TELEPHONE (Include Area Code)	22c. OFFICE SYMBOL AFGL/LWG

sub 2

+ or -

SECURITY CLASSIFICATION OF THIS PAGE

→ difference between the T_0 and the free-air anomaly has the root mean square value 5.8 mgal. This result is reasonable in comparison with the accuracy ± 10 E of the GGSS gradient data. A crossover discrepancy analysis indicated that the GGSS gradient data could have the accuracy about 10 Eotvos. (jlc)

Foreword

This report was prepared by Wang Yan Ming, Research Associate, Department of Geodetic Science and Surveying at The Ohio State University. This research was sponsored by the Air Force Office of Scientific Research, Air Force Systems Command, Geophysics Laboratory, under Contract Number AFOSR F19628-86-K-0016, The Ohio State University Research Foundation Project 718188, project supervisor, Richard H. Rapp. The contract covering this research is administered by the Geophysics Laboratory, Hanscom Air Force Base, Massachusetts, with Dr. Christopher Jekeli, Scientific Program Officer.

Computer resources were provided by contract funds and by the funds supplied by the Instruction and Research Computer Center, through the Department of Geodetic Science and Surveying.

Acknowledgments

I am very grateful to Dr. Richard H. Rapp for his suggestions on this research project. I wish to thank Dr. Christopher Jekeli for his valuable comments and suggestions. I also thank Ms. Lisa Schneck for the typing of this report.

Accession For	
NTIS GRA&I	<input checked="" type="checkbox"/>
DTIC TAB	<input type="checkbox"/>
Unannounced	<input type="checkbox"/>
Justification	
By _____	
Distribution/	
Availability Code <input checked="" type="checkbox"/>	
Dist	Avail and/or Special
A-1	



1. Introduction

The airborne Gravity Gradiometer Survey System (GGSS) took the first test flight in the Texas/Oklahoma area, and the first results were published by (Brzezowski et al., 1988). The data released by the Air Force Geophysics Laboratory (Jekeli, circular letter 5, 1989) includes the gradients of the gravity of the earth measured along the east-west or south-north direction in 19 tracks. The GGSS gradient data are the reduced gravity gradients. The gravity gradients were measured by the GGSS and then the mean values of the measurements of each track were subtracted. It will be shown later that these reduced gravity gradients are the second-order derivatives of the disturbing potential plus biases. Therefore it is important to remove the biases in the GGSS gradient data, before they are used for recovering the gravity disturbance.

The GGSS flew along the east-west (west-east) or south-north (north-south) direction in the test area. This mission supplies the crossover discrepancies of the gravity gradients. These data are useful for the determination of the biases in the GGSS gradient data. Like the determination of the bias in the satellite altimeter data for each arc, the relative bias in the GGSS gradient data can be determined by adding some constraints to the crossover discrepancy. After the adjustment, the biases between the tracks are removed.

The recovery of the first-order derivatives of the disturbing potential from the second-order derivatives is in principle an integration procedure. In this procedure the absolute bias in the GGSS gradient data need to be removed, but not only the relative bias. The absolute bias in the GGSS gradient data can be determined, provided tie point values of the gravity gradient are given at the flight altitude. Actually no such tie point values are available, so the absolute bias cannot be determined and removed from the GGSS gradient data. Furthermore, the GGSS data varies quite fast in the area, therefore the crossover discrepancy are sensitive to the positioning error of the GGSS. Based on the above consideration we would say that the crossover discrepancy adjustment is not suitable for the removing of the biases in the GGSS gradient data. But this adjustment has another application: it indicates the accuracy of the measurement of the GGSS gradient data. This will be shown later in the paper.

In this paper we use linear integration to transform the components of gravity gradient T_{xy} , T_{yz} into the vertical derivative of the disturbing potential. Then the tie point values of the free-air anomaly on the ground are combined in a crossover discrepancy adjustment for the determination of the bias and tilt of each track. Finally, the vertical derivative of the disturbing potential is determined on the ground by using the fast Fourier transformation (FFT) and least squares collocation (LSC). The results are compared with the 4 km x 4 km point free-air gravity anomaly in the test area (Rapp et al., 1988).

2. Variation of the gradient of the normal gravity in a local area

The gravitational potential of the earth W is usually split into the normal and disturbing potential (Heiskanen and Moritz, 1967, p. 82):

$$W = U + T \quad (1)$$

where U is the normal potential and T is the disturbing potential.

The local coordinate system xyz (North-East-Down) is often used for the GGSS. The gravity gradient W_{ij} is measured in the xyz coordinate system and has the form:

$$W_{ij} = U_{ij} + T_{ij} \quad i, j = 1, 2, 3 \quad (2)$$

where the subscripts i, j denote the derivatives of the potential and the numbers 1, 2 and 3 corresponding to the coordinates x, y, z respectively, e.g.,

$$W_{13} = \frac{\partial^2 W}{\partial x \partial z} = W_{xz}, \quad (3)$$

and so on.

Because the GGSS measures only the gravity gradient W_{ij} , we need to know the normal gravity gradient U_{ij} and this can always be done by taking account of the reference gravity field.

The reference gravity field is chosen as a normal gravity field (ibid, section 2-7):

$$U = V + \frac{1}{2} \omega^2 r^2 \cos^2 \theta \quad (4)$$

where V is the normal gravitational potential; ω is the angular velocity of the earth's rotation; r is the distance between the computed point and the geocenter of the earth and θ is the polar distance of the computed point from the north pole (cf. ibid., p. 18, Figure 1-7).

As an approximation we can take the normal potential as follows (cf. ibid, eq. (2-92) or (2-134a)):

$$U = \frac{kM}{r} - J_2 kM \frac{a^2}{r^3} \left(\frac{3}{4} \cos 2\theta + \frac{1}{4} \right) + \frac{1}{2} \omega^2 r^2 \cos^2 \theta \quad (5)$$

where k is the gravitational constant and M the mass of the earth.

In the spherical coordinate system we have the derivatives of the normal potential in the first order:

$$U_r = -\frac{kM}{r^2} + 3 J_2 kM \frac{a^2}{r^4} \left(\frac{3}{4} \cos 2\theta + \frac{1}{4} \right) + \omega^2 r \cos^2 \theta$$

$$U_\theta = \left(\frac{3}{2} J_2 kM \frac{a^2}{r^3} - \frac{1}{2} \omega^2 r^2 \right) \sin 2\theta$$

$$U_\lambda = 0, \quad (6)$$

and the derivatives of the normal potential in the second order are given by:

$$U_{rr} = 2 \frac{kM}{r^3} - 12 J_2 kM \frac{a^2}{r^5} \left(\frac{3}{4} \cos 2\theta + \frac{1}{4} \right) + \omega^2 \cos^2 \theta$$

$$U_{r\theta} = - \left(\frac{9}{2} J_2 kM \frac{a^2}{r^4} + \omega^2 r \right) \sin 2\theta$$

$$U_{\theta\theta} = \left(3 J_2 kM \frac{a^2}{r^3} - \omega^2 r^2 \right) \cos 2\theta$$

$$U_{r\lambda} = 0$$

$$U_{\theta\lambda} = 0$$

$$U_{\lambda\lambda} = 0 \tag{7}$$

Usually, the airborne flight is at an almost constant altitude above the sea level, and the flight area is not exceeded by a few degrees of latitude and longitude. Thus, the second-order derivatives of the normal potential can be written in a linear form:

$$U_{\pi} = U_{\pi}^0 + U_{\pi r}^0 \Delta r + U_{\pi\theta}^0 \Delta \theta$$

$$U_{r\theta} = U_{r\theta}^0 + U_{r\pi\theta}^0 \Delta r + U_{r\theta\theta}^0 \Delta \theta$$

$$U_{\theta\theta} = U_{\theta\theta}^0 + U_{r\theta\theta}^0 \Delta r + U_{\theta\theta\theta}^0 \Delta \theta$$

$$U_{r\lambda} = 0$$

$$U_{\theta\lambda} = 0$$

$$U_{\lambda\lambda} = 0 \tag{8}$$

where $\Delta r = r - r_0$, $\Delta \theta = \theta - \theta_0$, r_0 and θ_0 are the coordinates of the inertial point which can be defined as any point at the beginning of the GGSS mission. The superscript "0" denotes the values of the derivatives of the normal potential at the inertial point.

The non-zero third-order derivatives of the normal potential are given by:

$$U_{\pi\pi} = - \frac{6kM}{r^4} + 60 J_2 kM \frac{a^2}{r^6} \left(\frac{3}{4} \cos 2\theta + \frac{1}{4} \right)$$

$$U_{\pi\theta} = - \left(- 18 J_2 kM \frac{a^2}{r^5} + \omega^2 \right) \sin 2\theta$$

$$U_{r\theta\theta} = - \left(9 J_2 kM \frac{a^2}{r^4} + 2\omega^2 r \right) \cos 2\theta$$

$$U_{\theta\theta\theta} = - \left(6 J_2 kM \frac{a^2}{r^3} - 2\omega^2 r^2 \right) \sin 2\theta \quad (9)$$

The relationship between the local coordinate system xyz (which has the inertial point as the origin) and the spherical coordinate system $r\theta\lambda$ is given by

$$\begin{cases} x = r_0(\theta - \theta_0) \\ y = r_0 \cos \theta (\lambda - \lambda_0) \\ z = r_0 - r \end{cases} \quad (10)$$

where $(r_0, \theta_0, \lambda_0)$ is the coordinate of the inertial point.

Because the differences $\Delta\lambda = \lambda - \lambda_0$ and $\Delta\theta = \theta - \theta_0$ are small for a local area, we have approximately

$$\cos \theta = \cos(\theta_0 + \Delta\theta) \approx \cos \theta_0 + \Delta\theta \sin \theta_0 \quad (11)$$

If we choose $\Delta\theta < 3^\circ = 0.05$ rad, then the last term in (11) can also be omitted, and eq. (10) becomes:

$$\begin{cases} x = r_0(\theta - \theta_0) \\ y = r_0 \cos \theta_0 (\lambda - \lambda_0) \\ z = r_0 - r \end{cases} \quad (12)$$

From (12) we have immediately

$$\begin{aligned} \frac{\partial}{\partial r} &= -\frac{\partial}{\partial z}, \quad \frac{\partial^2}{\partial r^2} = \frac{\partial^2}{\partial z^2}, \\ \frac{\partial}{\partial \theta} &= \frac{1}{r_0} \frac{\partial}{\partial x}, \quad \frac{\partial^2}{\partial \theta^2} = \frac{1}{r_0^2} \frac{\partial^2}{\partial x^2}, \\ \frac{\partial}{\partial \lambda} &= \frac{1}{r_0 \cos \theta_0} \frac{\partial}{\partial y}, \quad \frac{\partial^2}{\partial \lambda^2} = \frac{1}{(r_0 \cos \theta_0)^2} \frac{\partial^2}{\partial y^2} \end{aligned} \quad (13)$$

By using eqs. (8), (9) and (13); we get the variation of the gradient of the normal gravity in a local area:

$$\Delta U_{yy} = U_{yy} - U_{yy}^0 = 0$$

$$\Delta U_{xy} = U_{xy} - U_{xy}^0 = 0$$

$$\Delta U_{yz} = U_{yz} - U_{yz}^0 = 0$$

$$\Delta U_{xx} = U_{xx} - U_{xx}^0 = \frac{1}{r_0^2} (U_{\theta\theta} - U_{\theta\theta}^0)$$

$$= -U_{r\theta\theta}^0 \frac{z}{r_0^2} + U_{\theta\theta\theta}^0 \frac{y}{r_0^3}$$

$$\Delta U_{xz} = U_{xz} - U_{xz}^0 = -\frac{1}{r_0} (U_{r\theta} - U_{r\theta}^0)$$

$$= U_{r\theta}^0 \frac{z}{r_0} - U_{r\theta\theta}^0 \frac{y}{r_0^2}$$

$$\Delta U_{zz} = U_{zz} - U_{zz}^0 = U_{rr} - U_{rr}^0$$

$$= -U_{rr}^0 z + U_{r\theta}^0 \frac{y}{r_0}$$

(14)

where we have used $z = r_0 - r = -\Delta r$.

Eq. (14) shows that the gradients of the normal gravity do not change with longitude (y). But they vary with the latitude (x) and the altitude (z).

Now we give a concrete example to demonstrate the variation of the gradients of the normal gravity in a local area. Taking the values of the parameters (Moritz, 1988, p. 355):

$$J_2 = 108\,263 \times 10^{-8}$$

$$a = 6378137 \text{ m}$$

$$kM = 3986005 \times 10^8 \text{ m}^3 \text{ S}^{-2}$$

$$\omega = 7292115 \times 10^{-11} \text{ rad S}^{-1},$$

(15)

and assuming that $r_0 = a + 1000 \text{ m}$, $\theta_0 = 30^\circ$, $\lambda_0 = 0$, then we have

$$U_{rr}^0 = -1.44 \times 10^{-3} \text{ Eötvös/m}$$

$$U_{r\theta}^0 = -2.13 \times 10^1 \text{ Eötvös}$$

$$\begin{aligned}
U_{r\theta\theta}^0 &= -3.39 \times 10^7 \text{ Eötvös} \cdot \text{m} \\
U_{\theta\theta\theta}^0 &= 2.13 \times 10^{13} \text{ Eötvös} \cdot \text{m}^2
\end{aligned}
\tag{16}$$

Putting eq. (16) into eq. (14), we obtain

$$\begin{aligned}
\Delta U_{yy} &= 0 \\
\Delta U_{xy} &= 0 \\
\Delta U_{yz} &= 0 \\
\Delta U_{xx} &= 8.34 \times 10^{-7} z + 8.91 \times 10^{-8} x \\
\Delta U_{xz} &= 3.34 \times 10^{-6} z + 8.34 \times 10^{-7} x \\
\Delta U_{zz} &= 1.44 \times 10^{-3} z - 3.34 \times 10^{-6} x
\end{aligned}
\tag{17}$$

From eq. (17) we can see that the gradients of the normal gravity change a very little in a local area. For example, let $z = 300$ meters, $x = 300$ km, we then have

$$\begin{aligned}
\Delta U_{xx} &= 2.67 \times 10^{-2} \text{ Eötvös} \\
\Delta U_{xz} &= 2.50 \times 10^{-1} \text{ Eötvös} \\
\Delta U_{zz} &= -0.57 \text{ Eötvös}
\end{aligned}
\tag{18}$$

From eq. (18) we can see that only ΔU_{zz} has a little change in a local area, and other gradients of the normal gravity can be considered as constant.

Now we discuss some practical aspects. The test flight of a GGSS was taken in a local area. If the gradient data are collected for each track and the mean value is subtracted from these data, then we have the reduced gradient data as:

$$T_{ij}^0 = W_{ij} - \bar{W}_{ij} \tag{19}$$

where the overbar denotes the mean values of the gradient of the gravity for a track, W_{ij} is the observed gravity gradient and T_{ij}^0 is the reduced gradient of the gravity.

Based on the above discussion we have approximately

$$\bar{U}_{ij} = U_{ij} \tag{20}$$

then we obtain

$$\begin{aligned}
 T_{ij}^0 &= W_{ij} - \overline{U_{ij} + T_{ij}} \\
 &= W_{ij} - \bar{U}_{ij} - \bar{T}_{ij} \\
 &= T_{ij} - \bar{T}_{ij}
 \end{aligned}
 \tag{21}$$

Eq. (21) indicates that the reduced gradient data T_{ij}^0 is different from the real second-order derivatives of the disturbing potential T_{ij} by a constant \bar{T}_{ij} . Normally, the global average of the disturbing potential and its derivatives should approach zero, but the mean value of the T_{ij} of each track will not always be equal to zero. This is one of the causes of the bias in the GGSS gradient data.

3. Relationship Between First-order and Second-order Derivatives of the Disturbing Potential

The relationship between the first-order and second-order derivatives of the disturbing potential is given by (cf. Moritz, 1971, p. 13):

$$T_i = T_i^0 + \int_{P_0}^P (T_{xi} dx + T_{yi} dy + T_{zi} dz) \quad i = 1, 2, 3
 \tag{22}$$

Here T_i^0 is the initial value of T_i at the point P_0 and T_i refers to a current point P . Obviously, the constant bias in the gravity gradient data plays an important role. If we have a bias c in the data T_{xi} , then from eq. (22) we have

$$\delta T_i = \int_{P_0}^P c dx = c \cdot x
 \tag{23}$$

where x is the change of the x -coordinate of the curve $P_0 P$. Eq. (23) means that a bias in the gravity gradient data becomes a tilt in the gravity disturbance. Because the bias is different for each component of the gravity gradient data measured on each track, the gravity disturbances obtained by using the linear integration have different tilt. Before we put the gravity disturbances on each track together to get the gravity disturbances on the ground, the tilt of each track has to be removed.

4. Crossover Discrepancy Adjustment for Processing Aerial Gravity Gradient Data

A crossover discrepancy adjustment has been used for processing satellite altimeter data. At first glance it seems that the crossover discrepancy adjustment can be directly used to the gravity gradient data for removing the bias in the data. As in processing the satellite altimeter data, if only the crossover discrepancy and some constraints are used, the relative bias in data can be determined. The relative bias determination is useless for gravity gradient data. The gravity gradient has six components. If only the relative bias is removed from each component of the

gravity gradient for each track, there are still different biases in components of the gravity gradient data. The reduced data cannot be combined together to recover the gravity disturbance on the ground. Of course the absolute bias in the gradient data can be determined, provided other data can be used, e.g., the tie point values of the gravity gradient at the flight altitude, but this kind of data does not exist at present. Therefore the crossover discrepancy adjustment is not practical for the elimination the bias in the gradient data.

The bias in the gravity gradient data is a serious problem for recovering the gravity disturbance. In order to solve this problem, we transform the second-order derivatives of the disturbing potential into the first order. The absolute bias and tilt in the first-order derivatives of the disturbing potential can be removed by using the crossover discrepancy adjustment and the tie point values (gravity anomalies, deflections of the vertical, etc.).

In the following we consider using two components of second-order derivatives of the disturbing potential, T_{xz} and T_{yz} , to recover the vertical component of the gravity disturbance.

The test flight of the GGSS were taken along south-north (x) and west-east (y) directions. By using eq. (22) we have

$$T_z(x, y_j) = T_z(x_0, y_j) + \int_{x_0}^x T_{xz}(x', y_j) dx' \quad (24)$$

$$T_z(x_i, y) = T_z(x_i, y_0) + \int_{y_0}^y T_{yz}(x_i, y') dy' \quad (25)$$

where the subscripts i, j denote the tracks along west-east or south-north direction, respectively.

Assume that there are random errors and a constant bias in the gravity gradient data. Then eqs. (24) and (25) become:

$$T_z(x, y_j) + V(x, y_j) = T_z(x_0, y_j) + \int_{x_0}^x T_{xz}(x', y_j) dx' + b(y_j)(x - x_0) \quad (26)$$

$$T_z(x_i, y) + V'(x_i, y) = T_z(x_i, y_0) + \int_{y_0}^y T_{yz}(x_i, y') dy' + b(x_i)(y - y_0) \quad (27)$$

where V and V' are the errors in the T_z caused by random errors in the gravity gradient data, $b(y_j)$ and $b(x_i)$ are the bias in the gradient data.

Denote

$$I_{ij}^x = - \int_{x_0}^{x_i} T_{xz}(x, y_j) dx,$$

$$I_{ij}^y = - \int_{y_0}^{y_i} T_{yz}(x_i, y) dy,$$

$$\begin{aligned} b_i &= b(x_i), & b_j &= b(y_j) \\ a_i &= T_z(x_i, y_0), & a_j &= T_z(x_0, y_j), \end{aligned} \quad (28)$$

then eqs. (26) and (27) have the values at the point (x_i, y_j) :

$$l_{ij}^y + V'(x_i, y_j) = a_i - T_z(x_i, y_j) + b_i(y_j - y_0) \quad (29)$$

$$l_{ij}^x + V(x_i, y_j) = a_j - T_z(x_i, y_j) + b_j(x_i - x_0) \quad (30)$$

Eqs. (29) and (30) can be considered as observation equations. The "observed" quantities l_{ij}^x and l_{ij}^y , can be obtained directly by using the numerical integration of the components of the GGSS gradient data T_{xz} and T_{yz} . Subtract (30) from (29), to obtain the crossover discrepancy:

$$d_{ij} + V_{ij} = l_{ij}^y - l_{ij}^x = a_i - a_j + b_i(y_j - y_0) - b_j(x_i - x_0) \quad (31)$$

with $V_{ij} = V'(x_i, y_j) - V(x_i, y_j)$, $d_{ij} = l_{ij}^y - l_{ij}^x$.

Eq. (31) is the basic equation for the crossover discrepancy adjustment. The crossover discrepancy d_{ij} is given, the parameters a_i , a_j , b_i , and b_j will be determined. Like the crossover discrepancy adjustment for altimeter data, eq. (31) describes an indeterminate problem, because there is no track fixed. In order to remove the indeterminacy the tie point values are introduced.

Now we consider how many tie point values are needed for the crossover discrepancy adjustment. If there are only biases in eqs. (29) and (30), i.e., b_i and b_j are equal to zero, in principle one tie point value of the T_z is needed for the determination of absolute bias of each track. If the bias and tilt are determined for each track, three tie point values whose locations are not on the same line are needed at least. This is the same as the theorem of the determination of a plane: Three points not on the same line determine a plane.

We have assumed that the tie point values are errorless. In practice it is not the case. Therefore using more tie point values is more reliable than using merely necessary tie point values.

If we put the tie point values at the beginning and end of the tracks along south-north direction, by using eq. (29) we get:

$$\begin{aligned} d_i^k + V_i^k &= a_i + b_i(y_k - y_0) \\ i &= 1, 2, 3, \dots; & k &= 1, 2 \end{aligned} \quad (32)$$

with

$$d_i^k = (T_z)_i + l_{ik}^y, \quad V_i^k = V'(x_i, y_k) - V(x_i, y_k) \quad (33)$$

where $(T_z)_i$ is the tie point value, V_i is the measurement error, y_k is the y-coordinate of the tie point.

The parameters a_i, a_j, b_i, b_j can be determined by using least squares adjustment by using eq. (31) and (32) together.

Eqs. (31) and (32) can be written in matrix form:

$$D + V = AX \quad (34)$$

where

$$D = \begin{bmatrix} d_{11} \\ d_{12} \\ \vdots \\ d_1 \\ d_2 \\ \vdots \end{bmatrix}, \quad V = \begin{bmatrix} V_{11} \\ V_{12} \\ \vdots \\ V_1^1 \\ V_2^1 \\ \vdots \end{bmatrix}, \quad A = \begin{bmatrix} 1 & 0 & 0 & \dots & -1 & 0 & \dots \\ 1 & 0 & 0 & \dots & 0 & -1 & \dots \\ \vdots & & & & & & \\ 0 & 0 & 0 & \dots & 1 & 0 & \dots \\ \vdots & & & & & & \end{bmatrix},$$

$$X = \begin{bmatrix} a_1 \\ a_2 \\ \vdots \\ b_1 \\ b_2 \\ \vdots \end{bmatrix}$$

A least squares solution is given by

$$\hat{X} = -(A^T P A)^{-1} A^T P D \quad (35)$$

where A^T is the transpose of the matrix A and P is the weight matrix. P is chosen as a diagonal matrix which has the elements of the reciprocal of the standard error of the discrepancy d_{ij} and d_i^k .

5. Downward Continuation of the Gravity Disturbance from the Flight Altitude to the Ground by Using FFT and Least Squares Collocation

Suppose that the bias and tilt of the vertical derivatives of the disturbing potential are removed by using the procedure from section 4, then the reduced vertical component of the gravity disturbance has to be downward continued to the ground. For the downward continuation we can use the fast Fourier transformation (FFT) or least squares collocation (LSC).

The basic formula for the upward continuation problem is the Poisson's integral. In a planar approximation it is (cf. Heiskanen and Moritz, 1967, p. 240):

$$T_z = \frac{H}{2\pi} \iint \frac{T_z^*}{d^3} dx dy \quad (36)$$

where H is the flight altitude of the GGSS, d is the distance between the current point on the ground and the computed point at the flight altitude. T_z and T_z^* are the vertical components of the gravity disturbance at the flight altitude and on the ground, respectively.

Applying the Fourier transformation to eq. (36), we get

$$F \{T_z\} = e^{-2\pi\omega H} F \{T_z^*\} \quad (37)$$

where

$$\omega = \sqrt{u^2 + v^2}, \quad u, v$$

are the frequency variables; $F \{ \}$ denotes the Fourier transformation.

From eq. (37) we have

$$F \{T_z^*\} = e^{2\pi\omega H} F \{T_z\} \quad (37^*)$$

Eq. (37*) describes the downward continuation of the T_z to the ground, and it is used often for determining the vertical component of the gravity disturbance on the ground. In order to reduce the effect of the high frequencies of the error in downward continuation, some kinds of smoothing or filtering should be used.

Least squares collocation is used in two aspects. First, there are only a few tie point values given on the ground. They are often too sparse to use eq. (36) to be upward continued to the flight altitude. This can be done only by using least squares collocation.

Second, least squares collocation can also be used for the downward continuation of the derivatives of the disturbing potential from flight altitude to the ground. The basic formula for least squares collocation is given by (Moritz, 1980, p. 102):

$$\hat{s} = C_{st}(C_{tt} + C_{nn})^{-1} t \quad (38)$$

where t is the observation, C_{st} is the covariance between the computed quantity s and the observation t , C_{tt} is the covariance between the observations, C_{nn} is the covariance of the measurement error.

It is reasonable to choose the covariance function for the vertical component of the gravity disturbance as (cf. Moritz, 1971, p. 36; and 1980, p. 179):

$$C(P, Q) = \frac{C_0 b^2 (z + z' + b)}{\left[\rho^2 + (z + z' + b)^2 \right]^{3/2}} \quad (39)$$

where b is a constant, P, Q have the coordinates (x, y, z) and (x', y', z') , ρ is the distance between the points $(x, y, 0)$ and $(x', y', 0)$, the variance C_0 is the value of the covariance function $C(\rho, Q)$ for $P = Q$.

The airborne flights are at a constant altitude, so we have $z = 0$, $z' = \text{constant}$. Eq. (39) becomes:

$$C(P, Q) = \frac{C_0 b^2 (z' + b)}{\left[\rho^2 + (z' + b)^2 \right]^{3/2}} \quad (40)$$

The covariance function will be used for the upward and downward continuation of a harmonic function above the sea level.

6. Practical Consideration and Computation Procedure Description

The GGSS data were measured along the tracks oriented west-east and south-north. The mathematical study of this procedure is given in section 2 and the conclusion is that the data can be considered as the second-order derivatives of the disturbing potential plus a bias. Therefore, the most important problem in processing the GGSS gradient data is the bias problem.

By using the crossover discrepancy adjustment the relative bias in the components of the gravity gradient can be determined. If the absolute bias is to be determined, at least one tie point of the gravity gradients at the flight altitude is needed.

If there are different biases in the components of the second-order derivatives of the disturbing potential, we cannot combine all six components together to recover the gravity disturbance because the biases make the gradient data inconsistent for this recovery. On the other hand, the crossover discrepancy indicates the accuracy of the data. Usually the measurement error (e.g., positioning error, instrument error) can be split into systematic and random parts. In the same manner the errors in the gradient data can be split into systematic error which consists of the systematic measurement error and the bias for each track (cf. section 2), and random error. After the crossover discrepancy adjustment, the bias and the systematic measurement error are reduced, then the new crossover discrepancy d_{ij} is equal to the difference of the random part of the measurement error in the gradient data:

$$d_{ij} = \epsilon_{ij}^{NS} - \epsilon_{ij}^{EW} \quad (41)$$

where ϵ_{ij}^{NS} , ϵ_{ij}^{EW} are the random part of the measurement errors of the gravity gradients along tracks oriented to north-south and east-west directions, the subscripts i, j denote the values and are located at the crossover of the tracks i and j .

Assume that the random measurement errors ϵ_{ij}^{NS} and ϵ_{ij}^{EW} are uncorrelated, then the RMS value of the discrepancy d_{ij} is equal to

$$\left(\sigma_{ij}^d \right)^2 = \left(\sigma_{ij}^{NS} \right)^2 + \left(\sigma_{ij}^{EW} \right)^2 \quad (42)$$

where σ_{ij}^{NS} and σ_{ij}^{EW} are the standard random measurement errors of the tracks along north-south and east-west directions; σ_{ij}^d is the RMS value of the crossover discrepancy between tracks i and j .

Therefore, the RMS value of the crossover discrepancy indicates the measurement accuracy of the gradient data.

In Table 1 we give the statistics of the crossover discrepancy for the GGSS gradient data before and after the crossover discrepancy adjustment. This table shows that the accuracy of the GGSS gradient data is around 10 Eötvös.

Table 1
Statistics of the Crossover Discrepancy of the GGSS Gradient Data
Unit Eötvös

		T_{xx}	T_{xy}	T_{xz}	T_{yy}	T_{yz}	T_{zz}
before adjust.	mean	-3.8	-4.4	-2.4	-3.6	-0.2	7.4
	max	37.5	35.2	28.3	38.8	38.0	58.6
	min	-36.9	-32.1	-36.1	-48.3	-55.6	-40.5
	RMS	14.4	13.1	12.1	16.6	17.9	19.4
	STD	13.9	12.3	11.9	16.2	17.9	17.9
after adjust.	mean	-0.0	-0.0	-0.0	-0.0	0.0	0.0
	max	34.6	41.7	27.9	30.6	54.9	32.9
	min	-28.6	-29.5	-26.1	-32.0	37.7	-32.4
	RMS	12.2	11.2	9.7	12.6	13.9	14.2
	STD	12.2	11.2	9.7	12.6	13.9	14.2

Usually the gravity anomaly rather than the gravity disturbance is given in an area. The relationship between the free-air anomaly and the vertical component of the gravity disturbance is given by (Heiskanen and Mortiz, 1967, p. 89):

$$\Delta g = T_z - \frac{2T}{R} \quad (43)$$

Notice that the axis z is in the opposite direction of the radius vector r . As first approximation we ignore the last term in eq. (43) and do not distinguish the free-air anomaly and the vertical component of the gravity disturbance.

In the test area (Texas/Oklahoma) 4 km x 4 km point free-air anomaly data are available. Therefore we transformed the components of the gradient data T_{xz} and T_{yz} into the vertical component of the gravity disturbance T_z by using the linear integration. Then the tie point values of the free-air anomaly were used to determine the bias and tilt in the T_z for every track. The computation procedure is described as follows.

a. Taking linear integration of the components T_{yz} and T_{xz} along south-north (x) and west-east (y) directions, the formulas (24) and (25) were used;

b. The 4 km x 4 km point free-air anomaly are given in the test area. Let the tie points have the coordinates (x_i, y_i, z_0) , $i = 1, 2, \dots, 20$, and $z_0 = 1$ km. Here x_i, y_i are the coordinates of the tie points located at the beginning and end of the tracks along the south-north direction in the square area (cf. Figure 1). The 4 km x 4 km point free-air gravity anomaly was interpolated at the points which have the coordinates (x_i, y_i) by using the bicubic spline function, then was upward continued to the flight altitude by using least squares collocation. The covariance function used is given by eq. (39).

- c. Using the tie point values of the free-air gravity anomaly and the crossover discrepancy to determine the bias and tilt for each track; the least squares adjustment (eq. (35)) was used;
- d. Using the bicubic spline function to interpolate the adjusted T_z at the flight altitude into a 2 km x 2 km grid interval, then fast Fourier transformation was used. As a comparison least squares collocation was used.

7. Results

The abridged airborne GGSS tracks are drawn in Figure 1. The data used for the analysis are constrained in the square area circled by thick lines. There are 19 tracks in which 9 tracks are along the east-west direction and 10 tracks are along the south-north direction. After the linear integration of the T_{xz} and T_{yz} along the south-north (x) and west-east (y) directions, l_{ij}^x , l_{ij}^y (cf. eqs. (24) - (28)) are given along each track. By combining the tie point values of the free-air gravity anomaly and the crossover discrepancy the absolute bias and tilt were determined for every track.

In the least squares adjustment solution, eq. (35) the weight matrix P has the elements $(10^2 \text{ mgal}^2)^{-1}$ for the crossover discrepancies and $(2^2 \text{ mgal}^2)^{-1}$ for the tie point values. The statistics of the crossover discrepancy are given in Table 2.

Table 2.
Statistics of Crossover Discrepancy of the T_z
Unit mgal

	max	min	mean	RMS	STD
Before adj.	82.56	-403.60	-109.13	157.39	113.39
After adj.	16.62	-17.55	-0.00	7.75	7.75

From Table 2 we can see that the crossover discrepancy is reduced enormously after the adjustment. Based on eq. (42) one can assess the accuracy of the T_z as about 5-8 mgal.

After the crossover discrepancy adjustment, T_z is given at the flight altitude. It can be analytically downward continued to the ground by using the fast Fourier transformation or least squares collocation. As a comparison both methods were used and the results are given in Table 3 and the following figures.

For the FFT computation a 2 km grid interval was used, then the results were averaged into 4 km x 4 km mean block values. For the least squares collocation computations the 4 km grid interval was used, and in the LSC solution 230 data points were used for the W-E tracks and 260 data points for the S-N tracks.

Table 3 shows the statistics of the differences between the free-air anomaly Δg and the vertical derivatives of the disturbing potential T_z which is recovered by processing the GGSS gradient data. This comparison may be somehow questionable, because the free-air anomaly and the T_z are not the same quantities. Even so, the difference between them (the last term in eq. (43)) is small in comparison with the free-air anomaly and Table 3 can still give us a general idea about the quality of the recovering of the T_z from the GGSS data.

Table 3

Statistics of the Differences Between Δg and T_z in Test Area
Unit mgal

	method	max	min	mean	RMS	STD
$\Delta g - T_z$ (W-E)	FFT	36.95	-17.54	2.47	8.60	8.26
	LSC	17.92	-18.93	0.85	8.04	7.99
$\Delta g - T_z$ (S-N)	FFT	27.76	-20.19	2.27	8.75	8.45
	LSC	23.71	-19.65	2.29	7.96	7.62
$\Delta g - T_z$ (all)	FFT	24.14	-20.46	-1.77	7.70	7.49
	LSC	14.73	-16.93	1.49	5.94	5.75

In Table 3 the T_z (W-E) and T_z (S-N) are the T_z obtained by using the data on tracks along west-east and south-north directions, respectively; T_z (all) is the T_z obtained by combining all T_z data on the flight altitude together.

Table 3 shows that both methods FFT and LSC are given almost the same results. The results are better if least squares collocation is used. The reason is that least squares collocation gives a smoother result than the fast Fourier transformation does. This will be clearly shown in the following Figures.

Figure 1 shows the abridged GGSS tracks. The data used for the analysis are confined inside the square area.

Figure 2 is the contour map of the free-air anomaly based on the 4 km x 4 km grid in the test area. The free-air anomaly varies significant along direction south-west to north-east.

Figure 3 and 4 shows the T_z recovered by using the T_z data on the tracks along west-east directions. Figure 3 is the FFT solution and 4 is the LSC solution. Obviously, the LSC solution is smoother than FFT solution.

Figure 5 and 6 are the contour maps of the T_z obtained by using the T_z data on the tracks along south-north direction.

Figure 7 and 8 show the T_z recovered by using the T_z data on the tracks along west-east and south-north directions. Obviously, they are the best results.

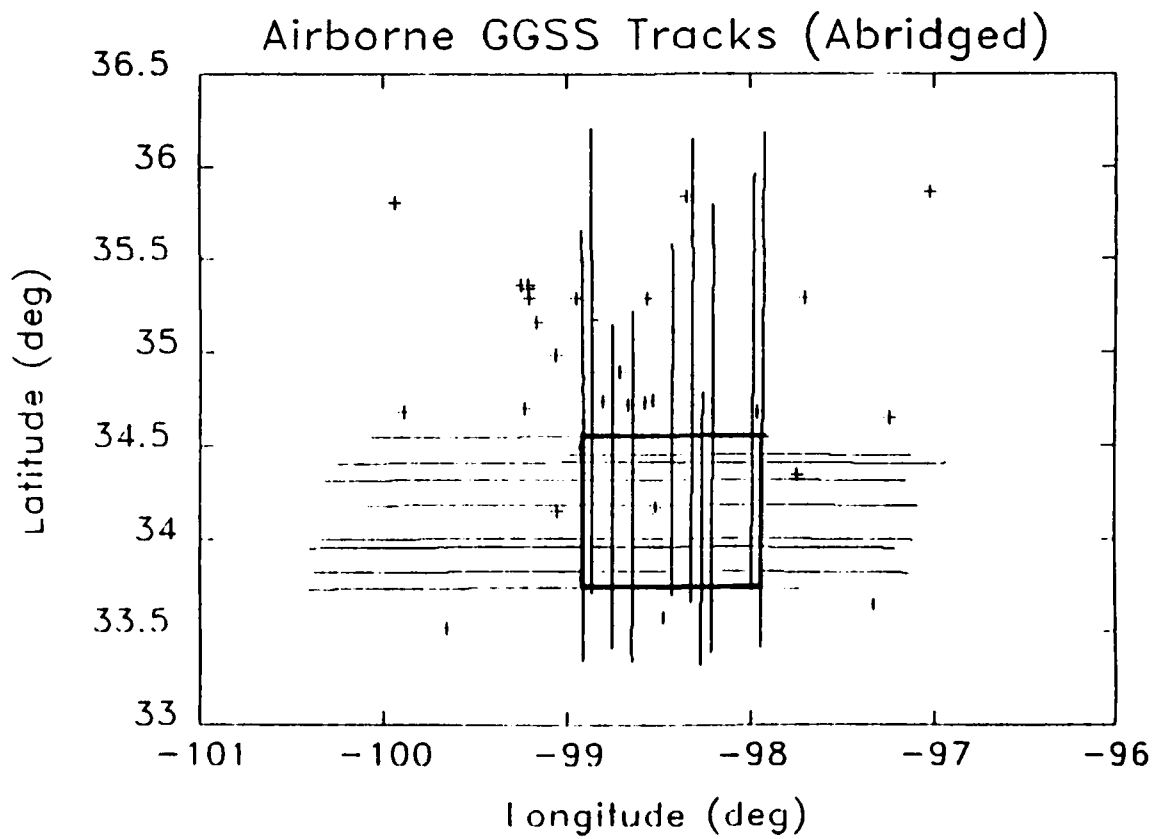


Figure 1. Location of the GGSS Tracks and the Test Area

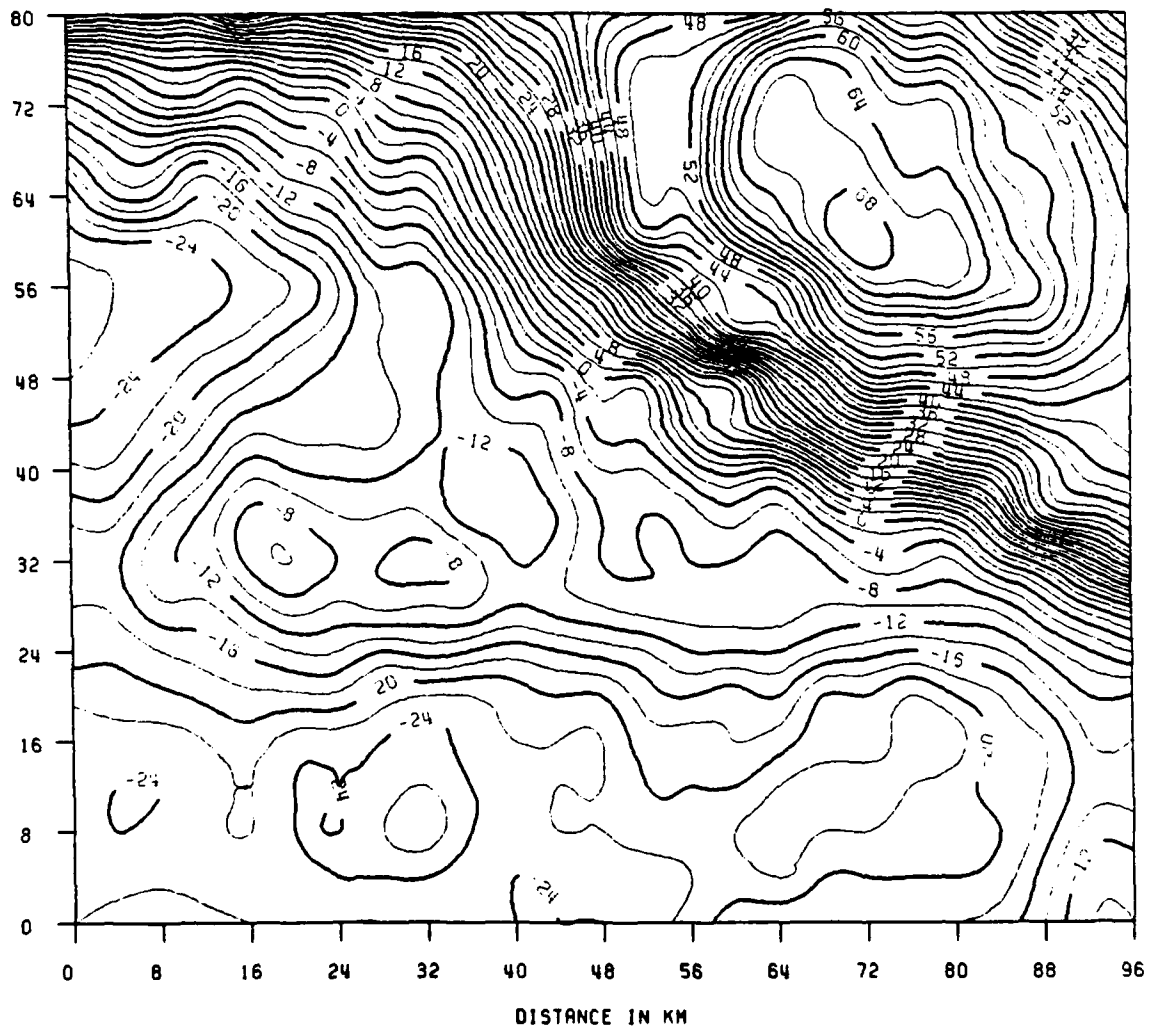


Figure 2. Contour Map of the Free-air Anomaly in Test Area

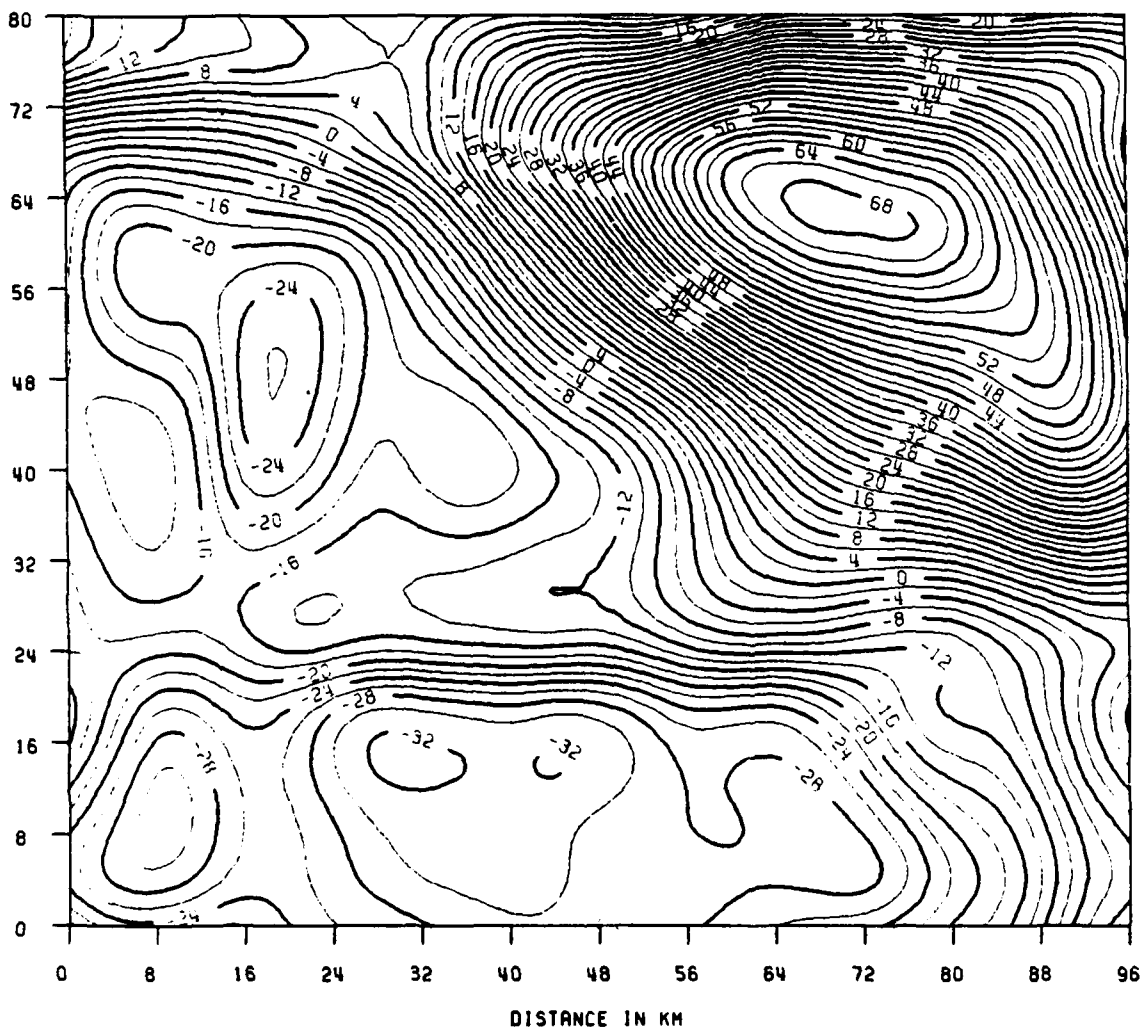


Figure 3. Contour Map of the T_z (W-E) FFT Solution

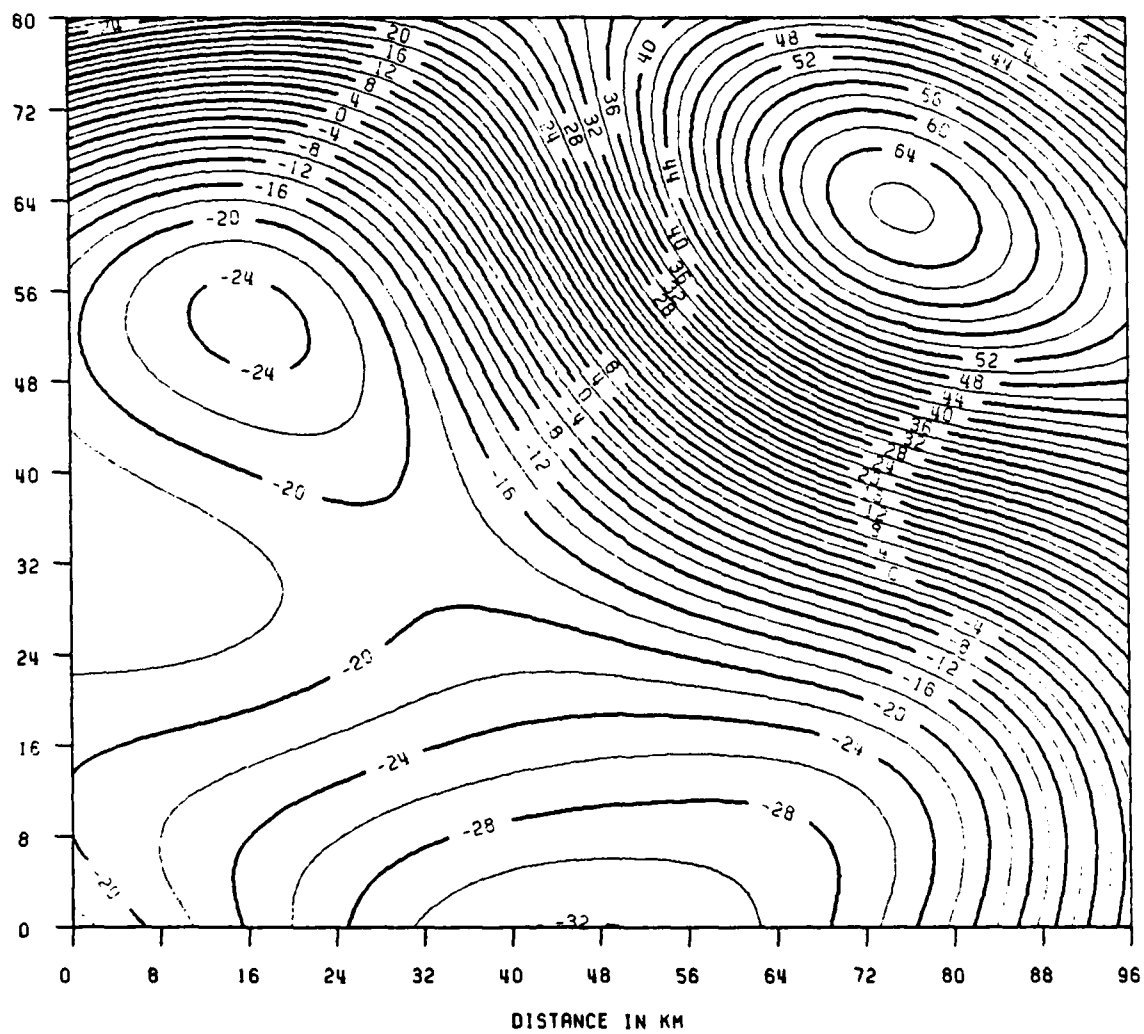


Figure 4. Contour Map of the T_z (W-E) LSC Solution

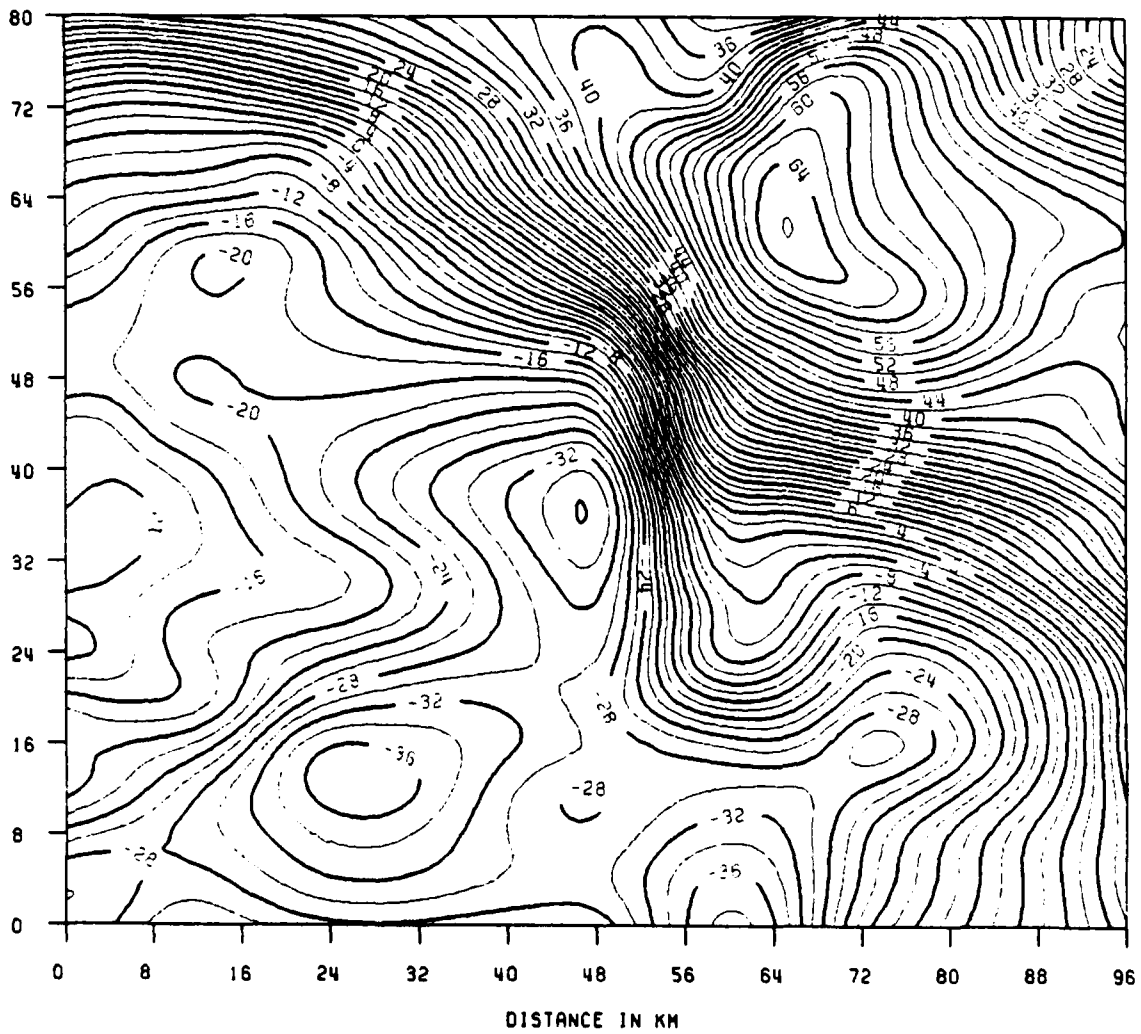


Figure 5. Contour Map of the T_z (S-N) FFT Solution

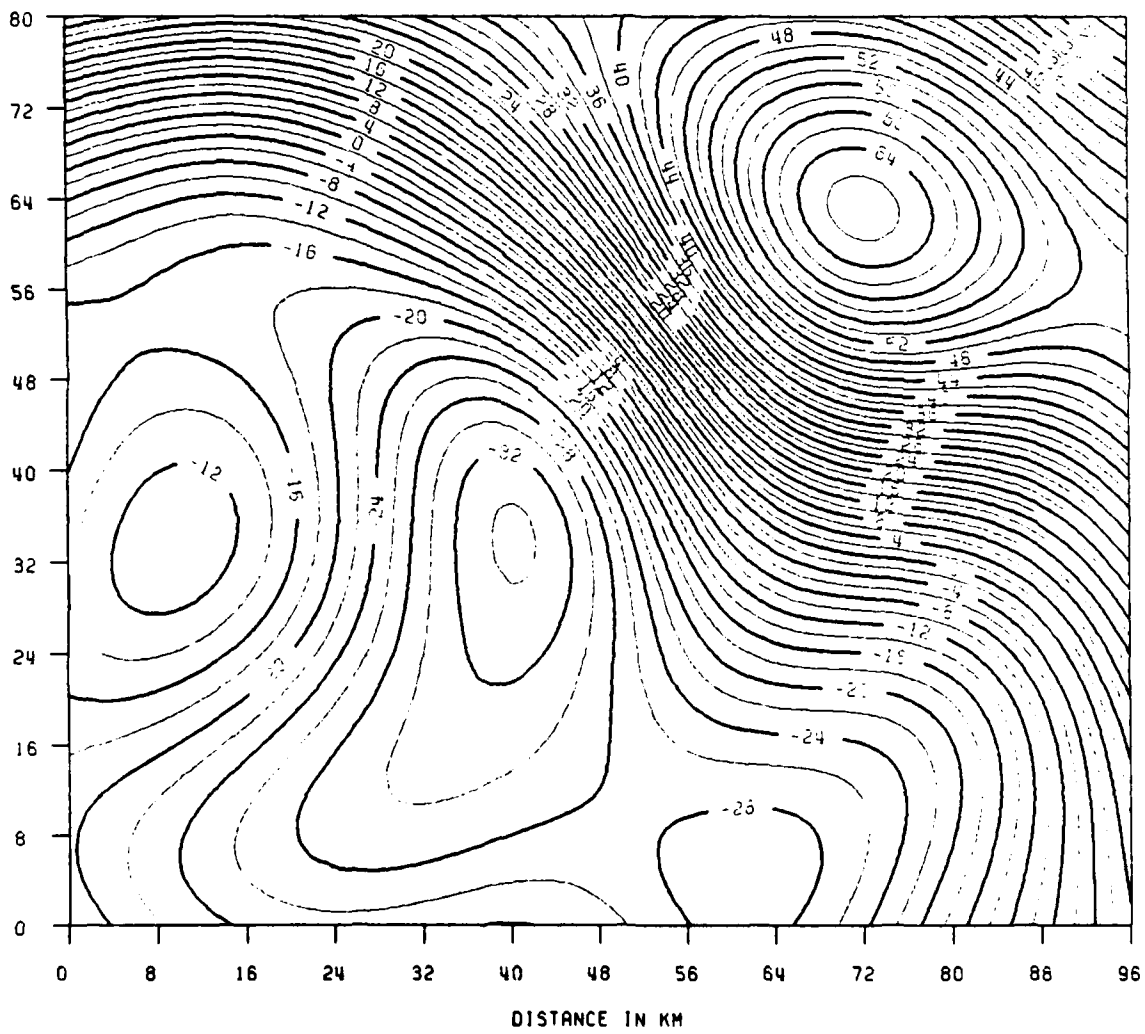


Figure 6. Contour Map of the T_z (S-N) LSC Solution

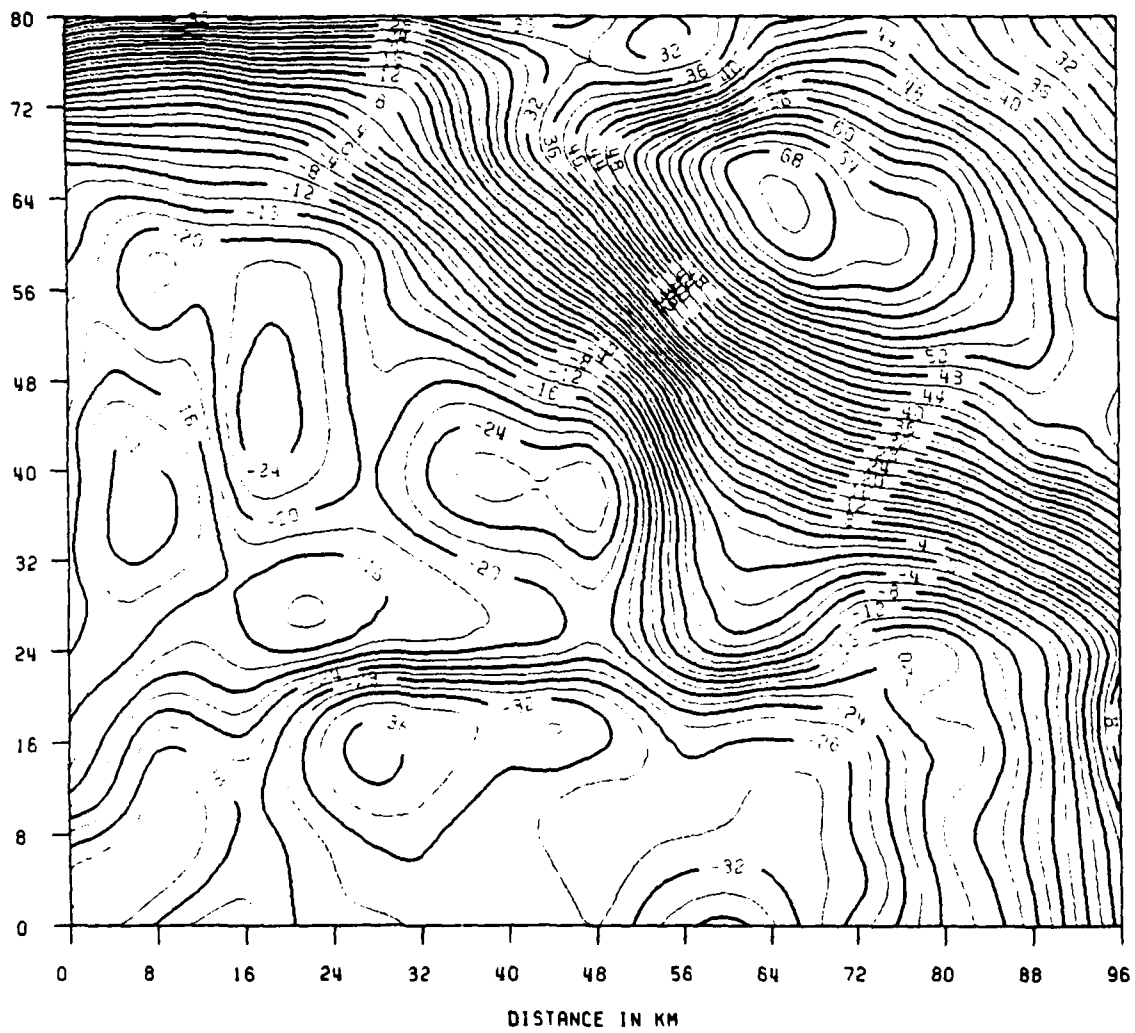


Figure 7. Contour Map of the T_2 (all) FFT Solution

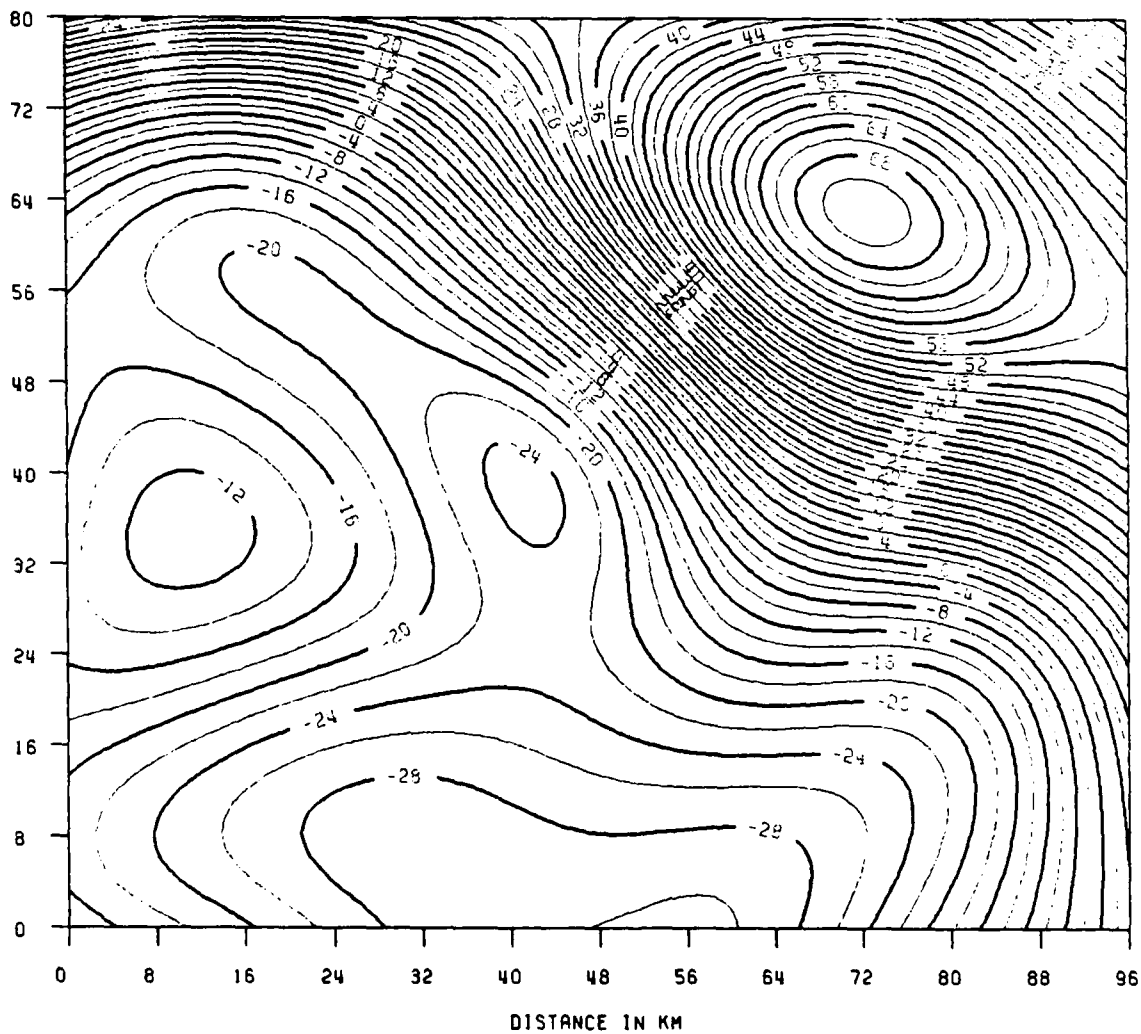


Figure 8. Contour Map of the T_z (all) LSC Solution

8. Conclusions and Recommendations

Because there are biases in the GGSS gradient data for different components of the gravity gradient and different tracks, this data cannot be directly used for recovering the gravity disturbance on the ground. In order to remove the bias in data, the crossover discrepancy adjustment and constraint equations can be used. By using the crossover discrepancy adjustment and constrain conditions, the relative bias in the data can be determined and removed. Even so the gradient data are difficult to be combined together to recover the gravity disturbance, because the different biases exist in the components of the gravity gradient after the crossover discrepancy adjustment and they make the data inconsistent for the recovery of the gravity disturbance.

In this study we used the linear integration to transform the second-order derivatives of the disturbing potential T_{xz} and T_{yz} into the vertical derivative of the disturbing potential T_z , then the crossover discrepancy and the tie point values of the free-air anomaly were used to remove the bias and tilt in the T_z . The best result agrees with the free-air anomaly in the test area at the 6 mgal level (RMS difference). In comparison with the accuracy of the GGSS gradient data (the crossover discrepancy indicates that the GGSS gradient data could have the accuracy about 10 Eötvös), the accuracy of the T_z is reasonable.

In the computations, the FFT and LSC method were used; both gave almost the same results. The LSC solution is smoother than the FFT solution and agrees a little better with the free-air anomaly in the test area (cf. Table 3).

The weakness of the computation procedure is that only two components of the GGSS gradient data were used. In the crossover discrepancy adjustment for the T_z there were 20 tie point values used.

In principle, one tie point (one tie point has six components of the gradient data) is needed to determine the absolute bias in the gradient data. If such tie point values are available, the absolute bias in the gradient data can be determined and removed. The reduced gradient data can then be combined together to recover the three components of the gravity disturbance. Normally, there are measurement errors in the tie point values. More tie point values can also improve the results of the crossover discrepancy adjustment by using least squares adjustment. In the future, if we get the tie point values of the gravity gradient, then the gradient data can be used together to get better recovery of the gravity disturbance.

If the second-order derivatives of the disturbing potential are transformed into the first order, then the bias and tilt have to be determined for each track. In principle, three tie points (every tie point has the T_x , T_y and T_z three values) are needed to remove the bias and tilt in the gravity disturbance data. If the accuracy of the gradient data is poor, as is the case in our computations, more tie point values are needed to improve the computation accuracy.

By the way, the GGSS is still in development. The accuracy of the measurements will be improved. One can hope in the future that one can get accurate gravity disturbance on the ground by processing such kinds of data. If the GGSS measurements are accurate enough, only a few tie point values are needed and this makes the GGSS more efficient and useful.

9. References

Brzezowski, S., D. Gleason, J. Goldstein, W. Heller, C. Jekeli, and J. White, Synopsis of Earth Field Test Results from the Gravity Gradiometer Survey System, In: Chapman Conference on Progress in the Determination of the Earth's Gravity Field, Sept. 1988.

- Heiskanen, W.A., and H. Moritz, *Physical Geodesy*, W.H. Freeman, San Francisco, 1967.
- Jekeli, C., *Terrestrial and Airborne Gravity Gradiometry*, Circular Letter 5, 1989, I.A.G. SSG 3.111, Circular Letter 5, 1989.
- Moritz, H., *Kinematical Geodesy II*, Report No. 165, Department of Geodetic Science and Surveying, Ohio State University, Columbus, 1971.
- Moritz, H., *Advanced Physical Geodesy*, Herbert Wichmann Verlag, Karlsruhe, 1980.
- Moritz, H., *Geodetic Reference System 1980*, Bulletin Geodesique, Vol., 62, No. 3, 1988.
- Rapp, R.H., and S. Zhao, *The 4 km x 4 km Free-Air Anomaly File for the Continuous United States*, Internal Report, Dept. of Geodetic Science and Surveying, The Ohio State University, 1988.